



---

1 **Comparison of water-soluble and insoluble organic compositions attributing to different light**  
2 **absorption efficiency between residential coal and biomass burning emissions**

3 Lu Zhang <sup>1,2</sup>, Jin Li <sup>1</sup>, Yaojie Li<sup>1</sup>, Xinlei Liu <sup>1</sup>, Zhihan Luo <sup>1</sup>, Guofeng Shen <sup>1,\*</sup>, and Shu Tao <sup>1,3</sup>

4 1. *Laboratory for Earth Surface Process, College of Urban and Environmental Sciences, Peking*  
5 *University, Beijing 100871, China*

6 2. *Hong Kong Polytechnic University, Department of Civil & Environmental Engineering,*  
7 *Kowloon, Hong Kong, China*

8 3. *College of Environmental Science and Technology, Southern University of Science and*  
9 *Technology, Shenzhen 518055, China*

10

11 \* *Corresponding author: Dr. Guofeng Shen, Peking University, Email: gfshe12@pku.edu.cn*



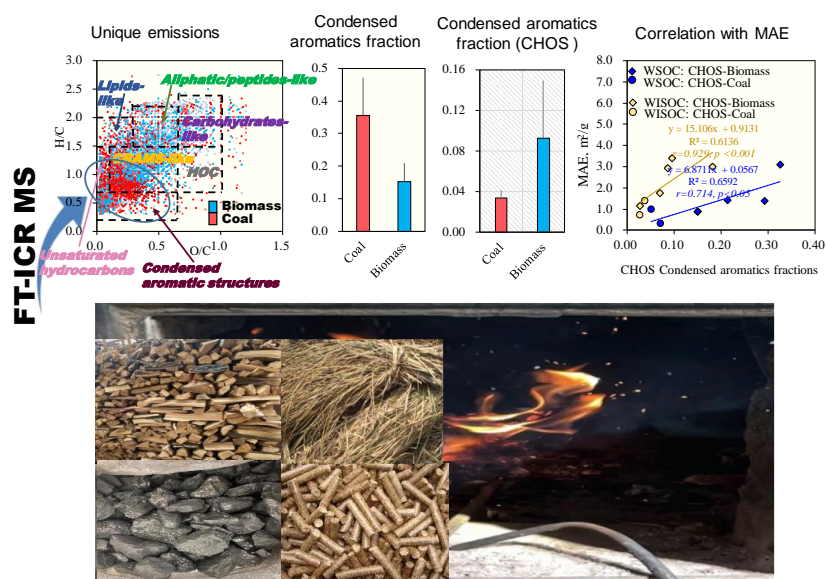
---

12 **Abstract**

13 There are growing concerns about the climate impacts of absorbing organic carbon (also known as  
14 Brown Carbon, BrC) in the environment, however, the chemical composition and association with  
15 the light absorption ability of BrC remain poorly understood. In this study, focusing on one major  
16 source of BrC, water-soluble and water-insoluble organic carbon (WSOC; WISOC) from residential  
17 solid fuel combustions were characterized at the molecular level, and evaluated for their quantitative  
18 relationship with mass absorption efficiency (MAE). The MAE values at  $\lambda=365$  nm from biomass  
19 burning were significantly higher than the coal combustion smokes. Thousands of peaks were  
20 identified in the  $m/z$  range of 150-800, with the most intense ion peaks of 200-500  $m/z$  for WSOC  
21 and 600-800  $m/z$  for WISOC, respectively. CHO group was the most abundant component in the  
22 WSOC extracts from biomass burning emissions compared to coals; while sulfur-containing  
23 compounds (CHOS+CHONS, SOCs) were more intense in the WISOC extracts, especially in coal  
24 emissions. Emissions of the CHON group were positively correlated with the fuel N content  
25 ( $r=0.936, p<0.05$ ), which explained higher CHON emissions in coal emissions compared to biomass  
26 burning emissions. The SOCs emissions were more predominant in flaming phases, as seen from a  
27 positive correlation between SOCs and modified combustion efficiency (MCE) ( $r=0.750, p<0.05$ ).  
28 The unique formulas of coal combustion aerosols were in the lower H/C and O/C regions with  
29 higher unsaturated compounds in the van Krevelen (VK) diagram. In WISOC extracts, coal  
30 combustion emissions had significantly high fractions of condensed aromatics (32-59%) which was  
31 only 4.3-9.7% in biomass burning emissions. The CHOS group in biomass burning emissions was  
32 characterized by larger condensed aromatic compound fractions compared to coal combustion. The  
33 CHOS aromatic compounds fractions were positively correlated with MAE values, in both WSOC  
34 ( $r=0.714, p<0.05$ ) and WISOC extracts ( $r=0.929, p<0.001$ ), suggesting the abundance of CHOS



35 aromatic compounds explained MAE variabilities across the different fuels.  
36 *Keywords:* light absorption properties, atmospheric aerosols, N-containing compounds, S-  
37 containing compounds, water-soluble compounds, water-insoluble compounds.  
38 **TOC**



39 **1. Introduction**

40 Light-absorbing organic carbon (OC), known as Brown Carbon (BrC), attracts growing  
41 concerns due to its direct radiative impact on climate change (Laskin et al., 2015; Wang et al., 2022).  
42 The global simulations suggested that BrC may contribute nearly 20% of the surface organic aerosol  
43 (OA) burden (Jo et al., 2016), and accounted for 19% of the light absorption by anthropogenic  
44 aerosols (Feng et al., 2013). BrC can be from various sources, including primary emission sources  
45 such as coal combustion, biomass burning, and vehicular emissions (Du et al., 2014; Olson et al.,  
46 2015; Bond, 2001; Sun et al., 2017; Chen and Bond, 2010). Secondary processes such as the  
47 oxidation of volatile organic compounds would also generate considerable BrC (Guan et al., 2020;  
48 Laskin et al., 2015). Among these sources, residential solid fuel burning produce large amounts of



---

49 BrC, accounting for 74% of the total anthropogenic primary emissions (Xiong et al., 2022).

50 Some efforts have been made to explore the BrC physiochemical properties in residential  
51 emissions. For example, water-soluble organic carbon (WSOC) and methanol-soluble organic  
52 carbon (MSOC) were analyzed in primary emissions from combustions of crop straw, wood fuel,  
53 and some coals (Park and Yu, 2016). Available studies suggested that the optical properties of  
54 primary BrC varied largely, being influenced by many factors, such as inherent fuel properties and  
55 combustion conditions. Mass absorption efficiency (MAE) is a key parameter in assessing direct  
56 radiative forcing of the light-absorbing carbonaceous aerosols (Huo et al., 2018). The water-soluble  
57 BrC from bituminous coals were found to have higher MAE values than anthracites (Tang et al.,  
58 2020); however, less well understood are the chemical components, at the molecular level,  
59 responsible for light absorption differences among different fuels. It was also reported that the mass  
60 absorption of water-insoluble organic carbon (WISOC) could be even greater than that of the water-  
61 soluble ones (Chen and Bond, 2010; Huang et al., 2018), but little information is available on  
62 chemical components of them. Considering that BrC light absorption varied dramatically among  
63 the different fractions and different fuels (Xie et al., 2017), detailed information of a comprehensive  
64 characterization, including the chemical and optical characteristics of the BrC fractions (including  
65 both water-soluble and water-insoluble ones) from the combustion source, is needed.

66 In this study, WSOC and WISOC in smoke particles produced from the burning of coals with  
67 different maturity, raw biomass fuels and biomass pellets in traditional and improved stoves were  
68 investigated for their chemical compositions and light absorption abilities. The use of biomass pellet  
69 has been heavily promoted over the last several years to mitigate air pollutant emissions from  
70 traditional solid fuels, and emission characteristics from improved stoves could be different from  
71 traditional ones. Optical property variations were quantitatively assessed and analyzed for their



---

72 association with chemical components. Unique molecules and fingerprints for coal and biomass  
73 sources were discussed that is critical in pollution source appointment.

## 74 **2. Materials and methods**

### 75 2.1 Laboratory Combustion Emission Experiment

76 In this study, fourteen coals with different maturity, five biomass pellet, and twelve raw  
77 biomass were tested in two stoves (one traditional stove (TS) and an improve stove (IS)) in the  
78 laboratory combustion system. The thirty-four fuel-stove combinations are listed in the Table S1.  
79 The combustion tests were conducted in a designed system equipped with real-time gaseous  
80 pollutants including CO, CO<sub>2</sub>, hydrocarbons (HC), and nitrogen oxide (NO<sub>x</sub> including NO and NO<sub>2</sub>)  
81 online monitor (Thermo Scientific Inc., Bremen, Germany). PM<sub>2.5</sub> (particles with aerodynamic  
82 diameters ≤2.5 μm) was collected at a flow rate of 16.7 L/min with the quartz filters. Fuel properties  
83 including moisture, volatile matter content (V<sub>dat</sub>), ash content, lower heating value (LHV), and  
84 contents of C, H, N, and S are tested and listed in Table S1. Details of stove construction and  
85 combustion processes were available in Zhang et al., (2022). Modified combustion efficiency (MCE)  
86 was calculated by integrating the incremental concentrations of CO<sub>2</sub> and CO as:

$$87 \quad \text{MCE} = \frac{\text{CO}_2}{\text{CO}_2 + \text{CO}}$$

88 where CO<sub>2</sub> and CO are the excess molar mixing ratios of CO<sub>2</sub> and CO, respectively (Pokhrel  
89 et al., 2016). The MCE values indicate different combustion phases: approximately 1 during flaming,  
90 and 0.7-0.9 during smoldering (Yokelson et al., 1997)

### 91 2.2 Bulk carbon and UV-vis Absorption Spectra

92 For each sample, a 4.9 cm<sup>2</sup> was extracted ultrasonically with 10 mL Milli-Q water (18.2 MΩ)  
93 for 30 min, and then the supernatant was separated. The extraction process was repeated twice, and



94 the extracts were combined to obtain WSOC. The water extract was then filtered via 0.22  $\mu\text{m}$   
95 polytetrafluoroethylene (PTFE) filter. The insoluble PM components that remained on the sample  
96 filter were further freeze-dried and extracted with methanol via sonication and then filtered via a  
97 PTFE filter to obtain water insoluble fraction. The carbon content of WSOC was analyzed with a  
98 total organic carbon (TOC) analyzer (TOC-Lcph/cpn, SHIMADZU, Japan), and the WISOC were  
99 calculated as OC subtracting WSOC given that the methanol extraction efficiency for all combustion  
100 samples were up to 90% as proved previously (Zhang et al., 2022). The OC was measured using a  
101 thermal-optical analyzer (Sunset OC/EC analyzer) with an interagency monitoring of protected  
102 visual environments (IMPROVE) program.

103 The light absorption spectra of the water and methanol extracts were measured between 200  
104 nm and 600 nm by UV-vis spectrophotometer (UV-2600, Shimadzu, Japan) at a step size of 1 nm.  
105 MAE values of WSOC and WISOC at the wavelength of  $\lambda$  ( $\text{MAE}_{\lambda, \text{WSOC}}$ ;  $\text{MAE}_{\lambda, \text{WISOC}}$ ) were  
106 calculated as following equation (Li et al., 2019):

$$107 \quad \text{MAE}_{\lambda, \text{WSOC}} = A_{\lambda, \text{WSOC}} \times \ln(10) / (C_{\text{WSOC}} \times L); \quad \text{MAE}_{\lambda, \text{WISOC}} = A_{\lambda, \text{WISOC}} \times \ln(10) / (C_{\text{WISOC}} \times L)$$

108 where  $A_{\lambda, \text{WSOC}}$  and  $A_{\lambda, \text{WISOC}}$  is the light absorption value of WSOC extract and WISOC extract  
109 at a wavelength of  $\lambda$ , respectively; C is the concentration of WSOC (or WISOC), and L is the optical  
110 path length which is 0.01 m in this study. It is important to note that the reported light absorption of  
111 WISOC in this study were underestimated, while such underestimation is insignificant due to the  
112 high extraction efficiency. In this study, the MAE values of extractable OC at  $\lambda$  of 365 nm ( $\text{MAE}_{365, \text{WSOC}}$   
113 &  $\text{MAE}_{365, \text{WISOC}}$ ) were discussed.

114 Absorption Ångström exponent (AAE) values were determined based on the following  
115 equation (Li et al., 2019; Li et al., 2020):

$$116 \quad A_{\lambda} = K_{\lambda} \cdot \lambda^{-\text{AAE}}$$

117 where K is a constant and AAE is obtained through the linear regression of  $\lg(A_{\lambda})$  against  $\lg \lambda$



---

118 (Fig S1). Wavelength of 300-400 nm is chosen according to the published literature (Yue et al.,  
119 2022), and the goodness of fit for all the samples in this study is greater than an  $r^2$  of 0.99.

### 120 2.3 FT-ICR MS Analysis

121 The WSOC and WISOC extract from seven selected source samples were selected for further  
122 FT-ICR MS analysis. These samples included two coals (high volatile bituminous coal, HVB;  
123 medium volatile bituminous coal, MVB) combusted in TS, two raw biomass (rice straw and pine  
124 wood) combusted in TS, pine wood combusted in IS, and two biomass pellet (crop straw pellet and  
125 pine wood pellet) combusted in IS as noted in SI. Fourier-transform ion cyclotron resonance mass  
126 spectrometry (FT-ICR MS) has been successfully applied for molecular-level characterization of  
127 compounds (Bianco et al., 2018) due to its ultrahigh resolution and mass accuracy. ESI is well-  
128 adopted to characterize soluble aerosols, especially for the detection of polar, hydrophilic molecules  
129 like humic-like substances (HULIS)-type compounds (Wozniak et al., 2008), because it is a “soft”  
130 ionization technique generating minimal analyte fragments, and thus can detect intact molecules of  
131 compounds. Therefore, the negative ESI-FT-ICR was applied here to determine the molecular  
132 compositions of WSOC and WISOC from combustion samples from different solid fuels. The  
133 methanol extracts were evaporated to dryness under a gentle stream of nitrogen, and then dissolved  
134 with Milli-Q water. The WSOC and water-reconstituted WISOC were submitted to solid-phase  
135 extraction (SPE) using Bond Elut PPL (500 mg, 6 mL, Agilent, U.S.A.). Prior to the extraction, the  
136 PPL cartridges were sequentially conditioned with 12 mL methanol and 12 mL Milli-Q water  
137 containing 0.05% hydrochloric acid (HCl). The extract was adjusted to Ph=2 using HCl to remove  
138 inorganic ions and was then loaded onto the PPL cartridges at a rate of 5 mL/min. Cartridges were  
139 washed with 18 mL Milli-Q water containing 0.05% HCL to remove salt, and then dried under pure  
140 nitrogen. Analytes were eluted with 12 mL methanol, and the combined eluates were concentrated



---

141 to 1mL. Then the molecular characterization was conducted using a 15T SolariX XR FT-ICR MS  
142 (Bruker Daltonik GmbH, Bremen, Germany) in the negative ESI mode (ESI<sup>-</sup>). The capillary inlet  
143 voltage was set at -4.0 kV and ion accumulation time was set to 0.06 S. There were 300 continuous  
144 4 M data FT-ICR transients added to improve the signal to noise ratio. The FT-ICR MS was  
145 calibrated with 10 mmol/L sodium formate in advance, and internal standard calibration with  
146 soluble organic matter (known molecular formula) was performed after the test. Finally, <1 ppm  
147 absolute mass error was achieved. Data processing details are described in the Supporting  
148 Information (SI).

### 149 3. Result and discussion

#### 150 3.1 Optical characteristics of WSOC and WISOC

151 MAE is an important parameter reflecting the light absorption capability of the carbonaceous  
152 aerosols. The MAE<sub>365, WSOC</sub> of aerosols from residential source in this study ranged from 0.21 to 3.1  
153 m<sup>2</sup>/g with an average of 1.3±0.7 m<sup>2</sup>/g. MAE values of extractable OC in this study was lower than  
154 that of 11.3 m<sup>2</sup>/g for pure BC aerosols (Bond and Bergstrom, 2006) and also lower than that from  
155 the filter-based MAE values of OC of 0.16-13 m<sup>2</sup>/g from residential sources (Zhang et al., 2021b).  
156 A significant difference ( $p<0.05$ ) of MAE<sub>365, WSOC</sub> was observed among the different fuels (Fig.1).  
157 The MAE<sub>365, WSOC</sub> of raw biomass combustion derived aerosols averaged at 1.7±0.8 m<sup>2</sup>/g, which  
158 was significantly higher ( $p<0.05$ ) than those from coal smoke (0.93±0.44 m<sup>2</sup>/g) and biomass pellet  
159 smoke (1.2±0.6 m<sup>2</sup>/g). The MAE<sub>365, WISOC</sub> was in the range of 6.6±0.5 m<sup>2</sup>/g and at the average of  
160 2.0±1.3 m<sup>2</sup>/g. Obviously, the absorption capability was higher for the WISOC extract than the  
161 WSOC extract. This is thought to be associated with distinct chemical compositions of light-  
162 absorbing organics. It was noted that the WISOC had higher MAE values compared to the WSOC,  
163 which may be explained by the more hydrophobic PAHs and quinones (Chen and Bond, 2010). The





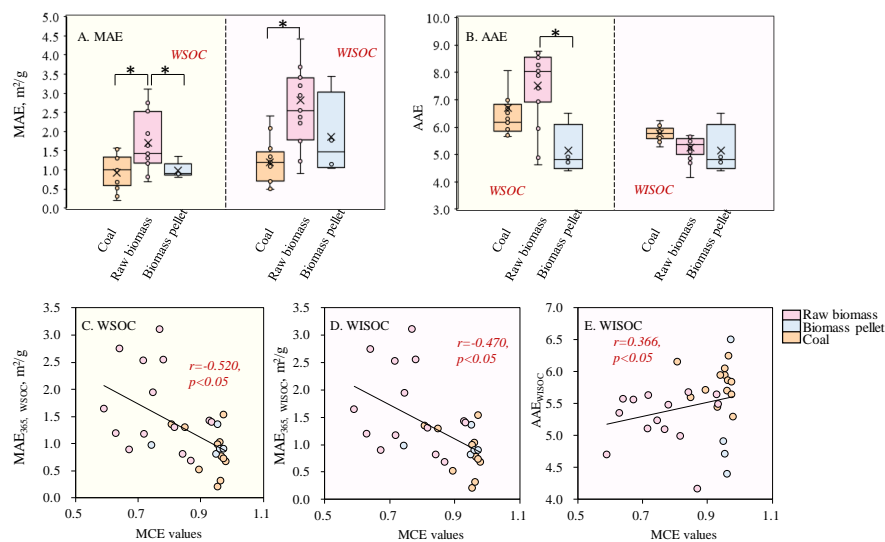
---

164 difference of  $MAE_{365, WISOC}$  among the different fuels was also statistically significant ( $p < 0.05$ ), as  
165 the value obtained from raw biomass burning ( $2.8 \pm 1.4 \text{ m}^2/\text{g}$ ) was significantly higher than that from  
166 coal combustion ( $1.2 \pm 0.6 \text{ m}^2/\text{g}$ ). The MAE values of soluble OC were dependent on the chemical  
167 composition of OC, that is, the chemical structure of the light absorbing chromophores and the ratio  
168 of non-light-absorbing organics to the chromophore components. The higher MAE values of raw  
169 biomass combustion derived aerosols might be caused by stronger light absorption capability of  
170 chromophores or higher ratio of chromophores. Our result was comparable to the published data,  
171 for example, the  $MAE_{365, WSOC}$  was reported to average at  $1.37 \pm 0.23 \text{ m}^2/\text{g}$  for biomass burning  
172 emissions (Park and Yu, 2016). The correlation of MAE with the MCE was investigated. The  
173 variability in MAE values, for both WSOC and WISOC, was observed to be negatively correlated  
174 with the MCE (or temperature as MCE was found to be positively correlated with the measured  
175 temperature in emission exhausts), when pooling all data together as seen in Fig. 1C and 1D.  
176 However, within each fuel group, there was no statistically significant correlation between the MAE  
177 and MCE values (Fig. S2). Some previous studies found that OC from wood pyrolysis under higher  
178 temperature conditions had stronger absorption capability (Chen and Bond, 2010; Saleh et al., 2014),  
179 but relatively higher mass absorption coefficient (MAC) values were also reported for the organic  
180 aerosol from wood combustion under the  $150^\circ\text{C} < T < 250^\circ\text{C}$  compared to emissions at a lower ( $T$   
181  $< 150^\circ\text{C}$ ) or higher ( $250^\circ\text{C} < T < 380^\circ\text{C}$ ) temperature condition (Rathod et al., 2017). Chen et al.,  
182 (2010) reported that that absorption per mass ( $\alpha/p$ ) of methanol extracts increased with increased  
183 wood pyrolysis temperature, but such increase was nonlinear and varied in burning emissions of  
184 different fuel types or wood with different sizes. Therefore, the apparently negative correlations  
185 between MAE and MCE values when pooling all data together in Fig. 1 were from distinct  
186 absorption properties of emissions from different fuel types, rather than the conditions like  
187 combustion temperature.



---

188 The AAE which indicates the wavelength dependence of light absorption is also an important  
189 parameter in climate models. The calculated AAE in the WSOC extract ( $AAE_{WSOC}$ ) ranged from  
190 3.8 to 11 with an average of  $6.9 \pm 1.5$ , and the difference of  $AAE_{WSOC}$  values among the different  
191 fuels was statistically significant ( $p < 0.05$ ) (Fig.1). The highest values were observed for the  
192 aerosols from raw biomass combustion of  $7.5 \pm 1.4$ , followed by coal smoke of  $6.7 \pm 1.5$  and biomass  
193 pellet smoke of  $5.6 \pm 1.2$ . The AAE values in the WISOC extract ( $AAE_{WISOC}$ ) were slightly lower  
194 than  $AAE_{WSOC}$ , which ranged from 4.2 to 6.5 with an average of  $5.5 \pm 0.5$ . The aerosols from biomass  
195 burning impact area was also reported to have higher  $AAE_{WSOC}$  of  $6.8 \pm 0.98$  than  $AAE_{WISOC}$  of  
196  $5.8 \pm 1.0$ . The differences of  $AAE_{WISOC}$  values among the different fuels were statistically  
197 insignificant ( $p > 0.05$ ), with averaged values of  $5.8 \pm 0.3$  for coal smoke,  $5.1 \pm 0.9$  for biomass pellet  
198 smoke, and  $5.2 \pm 0.4$  for raw biomass smoke. There was a weak positive correlation of  $AAE_{WISOC}$   
199 between the MCE values ( $p < 0.05$ ). The filter-based analysis also showed that AAE values were  
200 positively correlated with MCE values, indicating that more BrC were produced under smoldering  
201 phase compared with BC (Zhang et al., 2020). This study suggested that soluble BrC was apt to be  
202 generated during the smoldering phase in comparison with the non-light-absorbing OC. The AAE  
203 values in soluble OC in this study were higher than 4 for all samples, confirming the contribution  
204 of BrC to aerosol absorptivity from source emission. The result of this study was comparable to the  
205 published literature. For example, it was reported that the  $AAE_{WSOC}$  was in the range of 8.6-15 from  
206 coal combustion derived aerosols (Song et al., 2019), and 6.2-9.3 from biomass smoke (Park and  
207 Yu, 2016). The  $AAE_{WISOC}$  from wintertime urban aerosols were  $5.4 \pm 0.2$  in Xi'an and  $5.7 \pm 0.2$  in  
208 Beijing (Huang et al., 2020).



209 **Fig. 1** MAE values at  $\lambda=365$  nm (A) and AAE values (B) from the source samples (\* represents  
210  $p < 0.05$ ); Correlation between the MCE values with  $MAE_{365, WSOC}$  values (C),  $MAE_{365, WISOC}$  values  
211 (D), and  $AAE_{365, WISOC}$  values (E).

### 212 3.2 Molecular characteristics of WSOC and WISOC

213 The ESI-FT-ICR mass spectra of WSOC and WISOC samples are presented in Fig. 2.  
214 Thousands of peaks were identified in the  $m/z$  range of 150-800, indicating a complex chemical  
215 composition of aerosols from residential sources. Formulas detected in the raw biomass burning  
216 aerosols were significantly higher than those in biomass pellet and coal smokes (Fig. S3), which  
217 indicated a higher chemical complexity of raw biomass emissions. In addition, the combustion of  
218 pine wood in the improved stove generated less compounds, which was 93% peaks of that in the  
219 traditional stove (Table S2). The likely less complexity might be due to higher combustion  
220 efficiencies and temperature in the improved stove. Generally, higher levels of organic aerosols  
221 mass would be emitted during less efficient fuel burning, resulting from prolonged smoldering or  
222 incomplete burning (Holder et al., 2016). Our results suggested that corresponding higher chemical



---

223 complexity were also produced during the incomplete combustion in the traditional stove. The most  
224 intense ion peaks were distributed in the 200-500 m/z for WSOC, accounting for 58-86% of the  
225 total intensity. Similar results were also found in residential coal combustion (Song et al., 2019),  
226 biomass burning (Song et al., 2018), and ambient aerosols (Wozniak et al., 2008).

227 The mass spectra of WISOC are different from the WSOC, especially in aerosol emitted from  
228 coal combustion (Fig. 2). WISOC contained more molecules with larger m/z values of 600-800 in  
229 range, which indicated that WISOC extract had more compounds with higher MW than the WSOC  
230 extract. According to the molecular formulas and the intensity of each negative ion, the average  
231 molecular formulas for the WSOC were obtained with C atom from 20 to 24, H (21-29), N (0.32-  
232 0.75), O (5.6-7.0), and S (0.28-0.51) in the WSOC extract. All aerosols from biomass burning, either  
233 raw or pelletized ones, had higher relative O atom contents than coal smokes, indicating a higher  
234 oxidation degree of biomass emissions. For the WISOC, the average molecular formulas were  
235 assigned with 27-33 C, 26-35 H, 0.67-1.2 N, 6.6-11 O, and 0.34-0.92 S. The coal combustion  
236 derived aerosols had more C, N, and S atoms, but less H atom, compared with raw biomass. The  
237 combustion of biomass pellet also assigned with relative higher S elements. In addition, the WISOC  
238 fraction had a higher relative atom content than corresponding formulas of WSOC from the same  
239 source aerosol samples. These results indicated that in addition to the fuel type, extraction solvent  
240 also had important impact on the elemental composition of extractable BrC.



241 **Fig. 2** Negative ESI FT-ICR mass spectra of WSOC (A-G) and WISOC (A'-G') from the seven  
242 aerosol samples. Different formula groups were color-coded. The pie charts showed the relative  
243 intensities of different formula groups.

244 Molecular formulas identified by the FT-ICR-MS can be classified into 4 groups according to  
245 the elemental composition, including CHO (containing only C, H, O), CHON (hereafter similarly),  
246 CHOS, and CHONS. CHO was the most abundant group in the WSOC. The CHO group contributed  
247 51-67% to the total intensity in aerosols from raw biomass burning, which were significantly higher  
248 than those from biomass pellets (29-39%) and coal smokes (30-40%). The CHO compounds with  
249 oxygen-containing functional groups (e.g., hydroxyl, carbonyl, carboxyl, or esters) have been  
250 widely identified in both ambient aerosols (Jiang et al., 2021; Mo et al., 2022) and some source  
251 sample (Tang et al., 2020). These compounds contributed a broad range of proportions, from 43%

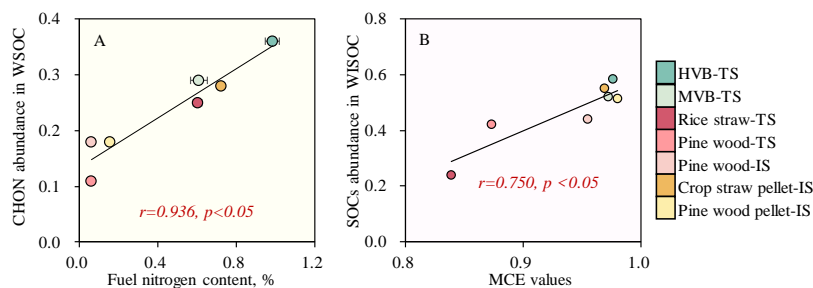


---

252 to 69% in residential biomass burning smokes (Tang et al., 2020), 9.7-48% in coal smokes (Song et  
253 al., 2019), and 20-39% in ambient aerosols (He et al., 2023) for the WSOC extract, which were  
254 comparable to ours. CHON compounds were also an important component in the aerosols,  
255 accounting for 29-36% in coal smokes, which were significantly higher than biomass burning  
256 smokes of 11-28%. One previous study reported that CHON species were more abundant in biomass  
257 burning smoke rather than the coal combustion ones (Song et al., 2018). This high fraction of CHON  
258 compounds in coal smokes might be caused by higher nitrogen content of coals as seen in Table S1.  
259 A strongly significantly positive correlation was found between the fuel nitrogen content and CHON  
260 species percentage ( $r=0.936$ ,  $p<0.05$ ) (Fig. 3). Such dependence was also found in the emission  
261 factors of  $\text{NO}_x$  ( $\text{NO}_x$  EFs) on fuel nitrogen content in our result (Fig. S4), as well as  $\text{NO}_x$ , HCN,  
262 and  $\text{NH}_3$  emissions reported by published literatures (Hansson et al., 2004). Sulfur-containing  
263 compounds (SOCs; including CHOS and CHONS) abundance was lower than CHO and CHON  
264 group, accounting for only 22-42% (13-30% for CHOS and 7.9-28% for CHONS, respectively).  
265 The fractions of SOC in the aerosols from coal combustion (25-42%) and biomass pellet burning  
266 (~42%) were comparable, but significantly higher than those from raw biomass (22-31%). The  
267 abundance of SOC was not statistically correlated with fuel S content in the present study for  
268 pooled data. However, when fuel subgroups were considered, fuels (coal or raw biomass) with  
269 higher sulfur content had higher SOC levels. Also, higher SOC emission was found for pine wood  
270 combusted in improved stove which have higher combustion efficiency than that in traditional stove.  
271 These results suggesting that except for fuel sulfur content, the fuel type and combustion efficiency  
272 would also influence the SOC emissions.



273 In the WISOC, intensities of these four groups among different source samples were different  
274 from that in the WSOC. The CHO group accounted for 27-45% in raw biomass burning aerosols,  
275 22-24% in biomass pellet smokes, and 13-22% in coal smokes. On the contrary, the SOCs  
276 abundance was significantly higher in WISOC, especially for the coals, accounting for 58% for  
277 HVB, and 52% for MVB. Significantly Positive correlation between the MCE values and SOCs  
278 abundance in the WISOC extract was found ( $r=0.750$ ,  $p<0.05$ ) (Fig. 3), while no clear association  
279 between fuel sulfur content and SOCs emissions observed in the WISOC. Combining the result  
280 from the WSOC extract, strong dependence of SOCs emissions on the combustion conditions were  
281 expected, while the fuel sulfur content had slight influence. Notably, the SOC abundance in aerosols  
282 from coal combustion was greatly higher than that in ambient aerosols (Lin et al., 2012), indicating  
283 that residential non-desulfurized coal combustion might be an important emitter of SOC in  
284 atmospheric samples. Thus, the CHON group emissions were determined mainly by the fuel  
285 nitrogen content, while SOCs emissions were strongly related to the combustion conditions (e.g.,  
286 flaming phase). It should be noted that the results of our analysis based on the current data without  
287 isotopic internal standard used were semi-quantitative, there are uncertainties that must be addressed.



288 **Fig. 3** Correlation between fuel nitrogen contents and abundances of CHON in WSOC (A), and  
289 the correlation between MCE values and the abundances of SOCs in WISOC (B).



---

290 3.3 Detailed CHO/CHON/CHOS/CHONS group differences across fuel types

291 Van Krevelen (VK) diagrams which can provide a visual interpretation of complex mass  
292 spectra can qualitatively identified chemical composition profiles in mixtures (Lv et al., 2016). The  
293 classification criteria of the VK diagram are provided in Table S3 (Patriarca et al., 2018; Tang et al.,  
294 2020). Fig. S5 and S6 show the VK diagrams of WSOC and WISOC. In both WSOC and WSOC  
295 extract, the carboxylic-rich alicyclic molecules (CRAMS-like) was the most abundant component,  
296 contributing to 53-69% in the WSOC extract and 37-56% in the WISOC extract, respectively. The  
297 condensed aromatics were also an important component in source samples, accounting for 7.3-13%  
298 in the WSOC, and for a higher proportion of 8.6-44% in the WISOC. This observation could be  
299 attributed to the hydrophobic property of condensed aromatic hydrocarbons, leading to a lower  
300 proportion in the highly polar WSOC. Among the identified formulas, 7.0-13% of total intensity in  
301 the WSOC and 3.6-17% in the WISOC were the aliphatic/peptides like compounds. Such fractions  
302 were comparable to unsaturated hydrocarbons with percentages of 3.9-15% in the WSOC and 2.0-  
303 11% in the WISOC. The compounds including lipids-like species and highly oxygenated  
304 compounds (HOC) were in a relatively lower abundance, with less than 10% each in the source  
305 samples. The different fuels showed varied chemical composition characteristics. Coal combustion  
306 aerosols had lower H/C ratios than those in biomass burning aerosols, indicating higher unsaturated  
307 degrees (Table S2). As indicated by the VK diagrams, the coal combustion produced a notable  
308 number of condensed aromatics, contributing to 27%-44% in the WISOC, which was significantly  
309 higher than that of 8.6-21% in the biomass burning emissions. The modified aromaticity index  
310 ( $AI_{mod,w}$ ) which is a measure of aromatic and condensed aromatic structure fractions and DBE  
311 values which is used as a measure of the unsaturated level in a molecule were all higher for coal  
312 emissions compared to the biomass emissions.





---

313 Distinct compound profiles being identified by the VK diagram classification criteria are  
314 consistent with discrepancies in the four (CHO/CHON/CHOS/CHONS) groups. For the CHO group,  
315 the most intense compounds were CARMs compounds with fractions of 69-84% in the WSOC  
316 extract and higher fractions of 51-80% in the WISOC extract. It was observed that raw biomass  
317 would emit slightly more CRAMs (76-84% and 61-80% in the WISOC) than coal (69-73% in the  
318 WSOC and 62-69% in the WISOC) and biomass pellet (70-75% in the WSOC and 51-56% in the  
319 WISOC) combustion. The condensed aromatic compound was also a crucial component, accounting  
320 for 13-20% in the WSOC and 19-27% in the WISOC of coal emissions. These fractions were  
321 significantly higher than those found in raw biomass (4.5-10% in the WSOC, and 7.9-10% in the  
322 WISOC) and biomass pellet (3.8-5.4% in the WSOC, and 11% in the WISOC) (Fig. 4). The other  
323 components accounted for a small (less than 10% each) of the total CHO intensity.

324 It was reported that the CHON compounds with  $O/N \geq 3$  might be the organonitrates candidate  
325 and nitro-substituted compounds, attributing to the allocation of one nitro ( $\text{NO}_2$ ) or nitrooxy ( $\text{ONO}_2$ )  
326 group (Bianco et al., 2018). In this study, the relative content of  $\text{CHON}_{O/N \geq 3}$  compounds (with  
327 respect to the overall CHON) in the biomass (raw and pellet ones) ranged between 71-82% and 85-  
328 91% for the WSOC and WISOC, which is distinctly lower than those found in coal smokes (86-90%  
329 for the WSOC, and 86-95% for the WISOC) (Table S4). Moreover, the  $\text{AI}_{\text{mod,w}}$  values for CHON  
330 compounds from coal combustion were higher than the biomass smokes for both WSOC and  
331 WISOC, as indicated by Table S2. It can thus be concluded that more CHON compounds with low  
332 aromaticity and a large amount of oxidized nitrogen functional groups were formed during the  
333 combustion of biomass fuels. Coal combustion emissions had more intense condensed aromatic  
334 compounds with percentage of 45-50% for the CHON group, which were significantly higher than  
335 those from raw biomass (4.5-37%) and biomass pellet burning (14-30%). This result confirmed the  
336 conclusion that the CHON compounds produced from the combustion of coals were characterized



---

337 by a relatively high aromaticity and a low degree of oxidation.

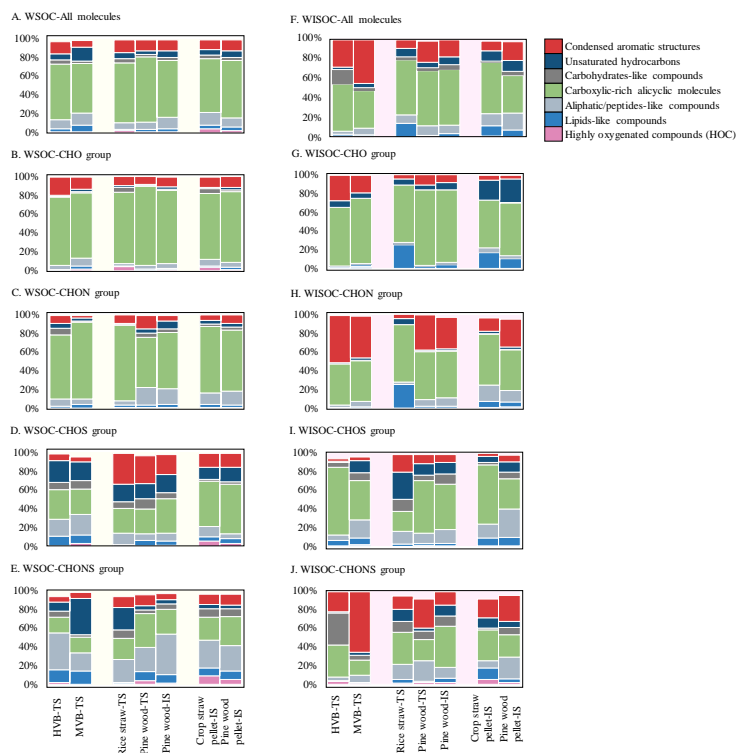
338 The O-rich CHOS fraction ( $O/S \geq 4$ ) accounted for 42–71% (concerning the overall CHON  
339 group) in the WSOC and 45-95% in the WISOC. O-rich CHOS fraction ( $O/S \geq 4$ ) content from coal  
340 (66-70% in the WSOC, and 78-98% in the WISOC) and biomass pellet (67-71% in the WSOC, 76-  
341 87% in the WISOC) were relatively higher than the raw biomass smoke (42-56% in the WSOC, and  
342 32-57% in the WISOC), suggesting that most of the CHOS compounds in coal and pellet smoke can  
343 be potentially assigned with more bearing sulfate ( $-\text{OSO}_3\text{H}$ ) or sulfonate ( $-\text{SO}_3$ ) groups. Different  
344 from CHO and CHON group, it was found that CHOS group in the biomass burning aerosols had  
345 much more intense condensed aromatic structure with percentage of 14-33% in the WSOC and 2.5-  
346 19% in the WISOC, especially for raw biomass (WSOC: 22-33%, WISOC: 8.5-19%), than coal  
347 combustion (WSOC: 4.9-7.0%, WISOC: 2.5-7.0%). For CHOS group in the WISOC extract, the  
348 unsaturated hydrocarbons were also an important component, accounting for 12-29% in raw  
349 biomass burning emissions, which were significantly higher than those in biomass pellet (6.9-11%)  
350 and coal (1.5-13%). These results indicated biomass burning emissions were characterized with  
351 higher unsaturation level and aromaticity for the CHOS group than coal combustion.

352 Nearly 34-85% of CHONS formulas have a large number of O atoms ( $\geq 7$ ), indicating the  
353 existence of  $-\text{NO}_3$  group (Table S4). These CHONS compounds are probably nitrooxy-  
354 organosulfates (Song et al., 2019). The remaining compounds (15-66%) of CHONS group had less  
355 than 7 atoms, implying that large amounts of CHONS compounds were assigned with reduced N  
356 (e.g., amide and nitrile, and heterocyclic aromatics). The condensed aromatic compounds identified  
357 by the VK diagram in the WISOC from coal combustion accounted for 22-64%, which were  
358 relatively higher than those from biomass burning (14-31%), indicating a higher degree of  
359 aromaticity. This was consistent with the difference observed in the  $\text{AI}_{\text{mod,w}}$  values as seen in Table



360 S2. The  $AI_{mod,w}$  of WISOC in coal emissions were 0.38 for HVB and 0.60 for MVB, and the values  
361 were higher than the raw biomass (0.32-0.38) and biomass pellet (0.35-0.36), confirming a higher  
362 aromatic compounds content of coal smoke sample than biomass for CHONS group.

363 Therefore, the CHO, CHON, and CHONS groups generated from coal combustion were  
364 characterized by high unsaturated level with more aromatic species, while CHOS groups had higher  
365 aromaticity degree in biomass smoke aerosols. Aromatic compounds might be the strong BrC  
366 chromophores contributing to light absorption (Song et al., 2019). The difference in MAE between  
367 coal and biomass emissions and association with the chemical components will be discussed in  
368 detail in the section 3.5.



369 **Fig. 4** Each component abundance identified by VK diagram of WSOC (A: all molecules, B: CHO  
370 group, C: CHON group, D: CHOS group, E: CHONS group) and WISOC (F: all molecules, G:  
371 CHO group, H: CHON group, I: CHOS group, J: CHONS group), the classification criteria was  
372 provided in the Table S3.



---

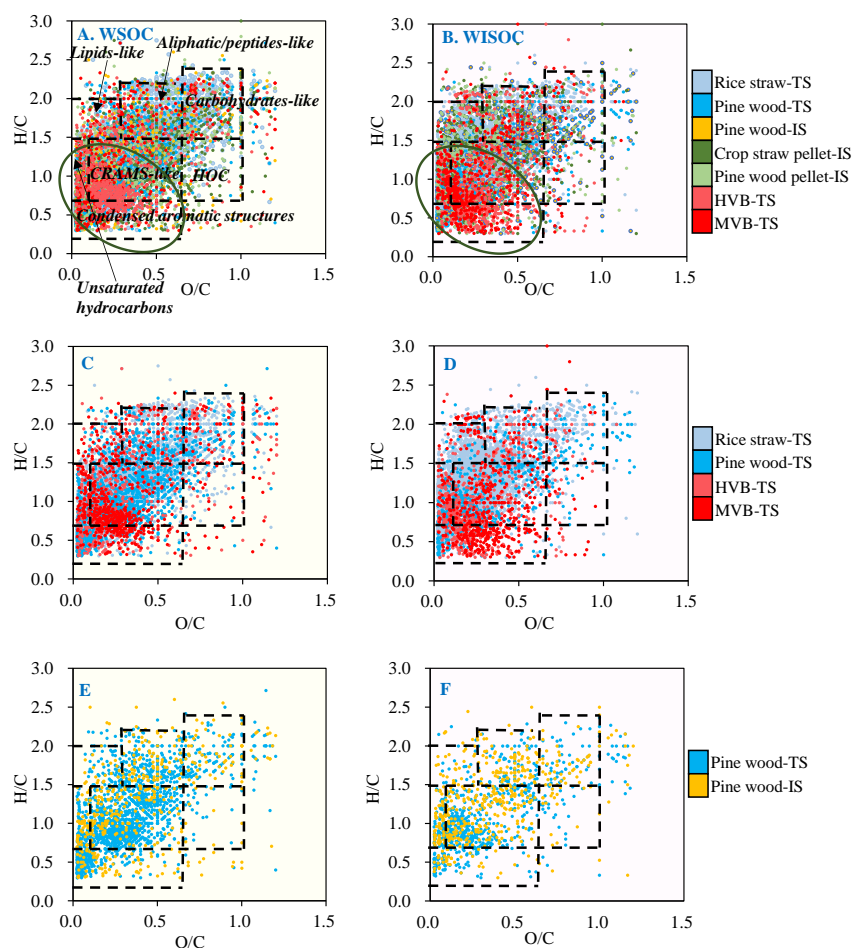
373 3.4 Likely unique molecules of biomass and coal combustion

374 The unique molecules may be inferred from the Venn diagram of formulas as shown in Fig. S7.  
375 Among the observed compounds, 3039 and 1624 unique molecular formulas were detected in the  
376 combustion of rice straw and pine wood in the traditional stove. These were significantly more than  
377 the unique formulas detected in biomass pellet-improve stove (638-696) and coal-traditional stove  
378 (570-734) in the WSOC fractions, suggesting a notable difference between the emissions from raw  
379 biomass and coal, even when using the same stove. Interestingly, fewer unique peaks were observed  
380 for pine wood-improved stoves (533), indicating that using an improved stove for raw biomass could  
381 narrow the difference between coal and biomass emissions. The similar trend was also found in the  
382 WISOC fractions (Fig. S7). The CHONS group accounted for a significant portion of unique  
383 formulas in source samples, particularly in coal smokes, representing 51-52% in WSOC and 51-69%  
384 in WISOC extract. The important role of CHONS group for unique emissions from coal combustion  
385 was also noted by Tang et al., (2020), who reported that CHO and CHON were the main component  
386 of unique molecular formulas of raw biomass burning emissions among the raw biomass burning,  
387 coal combustion and vehicle emissions, representing 88%-93%. This fraction was higher than our  
388 result of 33-77% in raw biomass and only 26-27% in biomass pellet. The distribution of the unique  
389 molecules further indicated substantial discrepancies among the fuels. Unique molecules in coal  
390 combustion derived aerosols were located in the region with lower H/C and O/C value compared  
391 with all other samples (Fig. 5) in both WSOC and WISOC extract, indicating a higher degree of  
392 unsaturation and lower level of oxidation. For example, it was observed that specific emissions from  
393 coal combustion were mainly composed by condensed aromatics (32-59%), followed by CRAMs  
394 compounds (23-39%) in WISOC extract. However, only 4.3-9.7% condensed aromatics of the total  
395 unique emissions were observed for biomass burning, with CRAMs being the main component (39-  
396 65%). As for different groups of CHO/CHON/ CHONS, the condensed aromatic compound contents



---

397 for all three groups in coal smoke aerosol (unique detected ones) were relatively higher than biomass.  
398 While CHOS group showed different trend that condensed aromatic compound contents of biomass  
399 smokes (unique detected ones) were relatively higher than coal smokes in WSOC extract and  
400 comparable to coal smokes in WISOC extract. This finding highlighted the CHOS group importance  
401 in distinguishing the aerosols from the combustion of coals or biomass, helping conduct the source  
402 apportionment of aerosols. Additionally, compared with the pine wood-improved stove emissions,  
403 most unique molecules in aerosol from pine wood-traditional stove combustion were in the region  
404 with lower H/C and O/C ratios (Fig. 5), which were identified mainly as CRAMs compounds. While  
405 the emissions from improved stove were distributed in a wider range with less CRAMs compounds  
406 and more aliphatic/peptides-like compounds observed. Unique molecules from biomass pellet  
407 combusted in improved stove distributed in the upper region of the VK diagram with higher H/C  
408 values in WISOC extract, which indicated a lower unsaturated degree (Fig. S8).



409 **Fig. 5** Van Krevelen diagrams of WSOC (left) and WISOC (right) from the source samples.  
410 Different color indicates unique formulas detected in each sample of solid fuel combustion.

411 A total of 484 molecular formulas were detected simultaneously in the seven aerosol samples  
412 in the WSOC extract and 306 in the WISOC extract. Among these commonly detected molecules,  
413 most of which were CHO compounds with the molecular numbers accounting for 60% and 73% in  
414 the WSOC and WISOC, respectively. CHON accounted for 31% of WSOC and 19% of WISOC,  
415 while SOCs only occupied about 10%. As seen in the Fig. S9, these CHO compounds were mainly  
416 composed of CRAMs-like compounds, and also several lipids-like and aliphatic/peptides-like



---

417 compounds. Moreover, these compounds were relatively small molecular compound assigned with  
418 8-28 C atom and 2-12 O atom with DBE values of 2-17 for the WSOC extract. The relatively more  
419 C atom assigned with larger DBE values was observed for the CHO compounds in WISOC, which  
420 could be partially explained by that the overall CHO compounds in the WISOC extract had larger  
421 MW values with a high degree of unsaturation. In total, the CHON compounds were also CRAMS-  
422 like compounds, and almost none compounds were expected to be aromatics. CHOS and CHONS  
423 species had much fewer formulas, especially for CHONS, only accounting for 1.0% in the  
424 commonly detected molecules in the WISOC. The unsaturated levels of commonly detected  
425 molecules in all seven source samples were relatively low. For example, the condensed aromatic  
426 compounds accounted for 6.5-9.3% and 3.3-4.1% of the total intensity for coal smoke and biomass  
427 smoke in the WSOC, respectively, as well as 0.38-8.3% and 18-21% in the WISOC extract.  
428 Different from the CHO, CHON, and CHONS group, high percentages of condensed aromatic  
429 compounds were found in CHOS group (commonly detected ones) from raw biomass burning  
430 aerosols with range of 6.6-51% in the WSOC and 12-46% in the WISOC extract. These fractions  
431 were significantly higher than those from coal smokes of 4.1-4.9% in the WSOC and 8.8-25% in  
432 the WISOC extract. Combining the finding that CHOS group in biomass smokes had a higher  
433 aromaticity degree in both WSOC and WISOC extract. However, the unique molecules in WISOC  
434 extract did not follow this trend. It was thus speculated that the higher aromaticity degree of CHOS  
435 group in biomass smokes was attributed to the intensity variation of these simultaneously detected  
436 compounds, rather than the unique emission from special source for the WISOC extract.

437 To explore the potential influence of fuel properties and combustion conditions on chemical  
438 composition, the major factors such as fuel moisture,  $V_{daf}$ , and parameters reflecting combustion  
439 conditions including MCE, EC/OC ratios were assessed. The liner correlation analysis was applied  
440 to estimate the effect of these factors on each molecular intensity (commonly detected ones)



---

441 (Fig.S10 and S11). The aliphatic compounds (including lipids like, aliphatic/peptides like and  
442 carbohydrates like compounds) were negatively correlated with the fuel moisture and positively  
443 correlated with  $V_{daf}$  and EC/OC ratios. Fuel moisture has been recognized as an important factor  
444 influencing pollutant formation, but the influence is usually very complicated. The observed  
445 relationship between fuel water content and pollutant EFs varies largely among studies, which may  
446 be attributed to factors such as different water contents, pollutant types, and interactions among  
447 other influencing factors. Fuels with high moisture levels may have high emissions, as extra energy  
448 is needed to vaporize water during the burning process; however, a decrease in combustion  
449 temperatures under very high-water content conditions may slow the pollutant formation rate and  
450 consequently lower emissions. Higher EC/OC ratios and larger MCE values tend to be associated  
451 with stronger flaming conditions. The results suggested that the aliphatic compounds were apt to be  
452 produced on the period of the flaming phase with higher combustion temperature. This result could  
453 partially explain that aliphatic/peptides like compounds would be apt to be produced in the improved  
454 stove rather than the traditional stove. In comparison, the emissions of CRAMs-like compounds  
455 which is the most abundant species were decreased with the increased MCE and EC/OC values,  
456 indicating that CARMs-like compounds were generated under smoking phase. No significant  
457 correlations of aromatics, unsaturated hydrocarbons, and HOCs were observed with these  
458 parameters, resulting from their small proportion in commonly detected molecules. It is worth  
459 noting that there may be significant differences, even for the same fuel, in chemical composition  
460 depending on other factors such as stove type and combustion conditions. The interactions among  
461 these factors making it difficult assessing their influence. It was found that only around 50%  
462 identified molecules were overlapped emissions for pine wood combusted in traditional stove and  
463 in improved stove, suggesting the importance of stove used. Fewer fraction of 25-30% molecules  
464 were observed compared the pine wood emissions with coals combusted in the same stove, which





---

465 suggested that the influence of varied fuels on chemical composition could surpass the differences  
466 caused by different stoves. Our previous studies have revealed that fuel type was the most important  
467 factor influencing on the MAE values (Zhang et al., 2021b) and BrC EFs (Zhang et al., 2021a). The  
468 present study highlighted the dominant effect of fuel type on the chemical composition of soluble  
469 OC, providing a theoretical basis for source appointment based on molecular composition.  
470 Moreover, the combustion conditions would have significant effect on the molecular intensity,  
471 resulting in differences in MAE eventually as indicated in the section 3.1.

### 472 3.5 The correlation of light absorption properties with molecular compositions

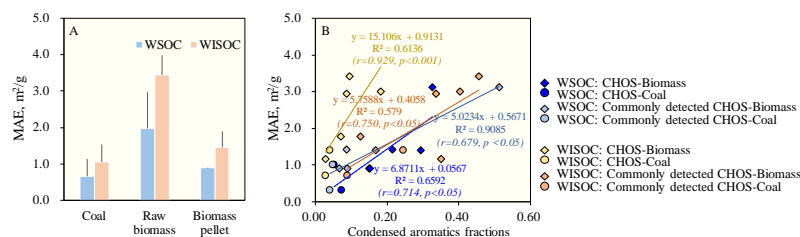
473 Here we specifically look into the variability in optical characteristics among the different fuels  
474 attributed to its chemical compositions. No significant correlations were observed between the AAE  
475 values of soluble OC and the molecular composition, indicating that AAE could be influenced by  
476 many factors. The MAE may be influenced by the degree of oxidation and unsaturation degree (Mo  
477 et al., 2017) (Tang et al., 2020), however, there was no significant correlation found between the  
478 MAE values and O/C values in the present source samples, implying that the BrC light absorption  
479 ability might not be directly affected by its oxidation degree.

480 The  $MAE_{365, \text{wsoc}}$  values were significantly positively correlated with the DBE values  
481 ( $r=0.786, p<0.05$ ) and the MW values ( $r=0.750, p<0.05$ ) (Fig. S12), indicating that unsaturation and  
482 MW played a crucial role in the light absorption capability of the source samples. In the above  
483 discussion, we have noticed that CHOS group in biomass was characterized by higher degree of  
484 aromaticity than coal smoke aerosol, while CHO, CHON, and CHONS group have a higher aromatic  
485 degree in the coal emissions. A significantly positive correlation ( $r=0.714, p<0.05$ ) was observed  
486 between  $MAE_{365, \text{wsoc}}$  values and the condensed aromatics percentages from the CHOS group (Fig.  
487 6), indicating that aromatics in CHOS group contributed to the high light absorption ability of



488 biomass smokes.

489 For the WISOC extract, no significant correlation was found between the MAE<sub>365, WISOC</sub> values  
490 with MW or DBE values, which might be explained by much different chemical composition for  
491 insoluble compounds compared with soluble parts. Although the coal combustion emitted much  
492 more aromatic compounds with higher DBE values for the WISOC, the MAE values were not  
493 significantly higher. The significantly positive correlation ( $r=0.929, p<0.05$ ) between MAE<sub>365, WISOC</sub>  
494 values and the CHOS condensed aromatics percentages confirmed the importance of CHOS  
495 aromatics in determining the light absorption capability from source samples. As mentioned in the  
496 Section 3.4, higher aromaticity degree of CHOS group in biomass smokes was largely due to the  
497 intensity variation of these commonly detected compounds in all source samples. The further  
498 analysis revealed that MAE<sub>365, WISOC</sub> values were positively correlated ( $r=0.750, p<0.05$ ) with the  
499 CHOS condensed aromatics fractions which were the fraction simultaneously detected in all  
500 samples. These results indicated that light absorption capability of source aerosols may be due to  
501 the higher abundance of some CHOS aromatic compounds commonly emitted from both coal and  
502 biomass, rather than the unique tracers.



503 **Fig. 6** MAE values at  $\lambda=365$  nm (A) and correlations between condensed aromatics fractions in  
504 CHOS and in commonly detected CHOS with MAE values (B) from the source samples

#### 505 4. Conclusion and implication

506 The MAE<sub>365, WISOC</sub> ranged from 0.21 to 3.1 m<sup>2</sup>/g with an average of 1.3±0.7 m<sup>2</sup>/g. The MAE<sub>365,</sub>  
507 WISOC was found to be higher with an average of 2.0±1.3 m<sup>2</sup>/g. There were significant differences



---

508 ( $p < 0.05$ ) observed among the different fuels for both  $MAE_{365, WSOC}$  and  $MAE_{365, WISOC}$ , as raw  
509 biomass burning combustion had significantly higher values than the coal combustion. The  
510  $AAE_{WSOC}$  ranged from 3.8 to 11 with an average of  $6.9 \pm 1.5$ . The  $AAE_{WISOC}$  were slightly lower than  
511  $AAE_{WSOC}$ , which ranged from 4.2 to 6.5 with an average of  $5.5 \pm 0.5$ . Thousands of peaks were  
512 identified in the  $m/z$  range of 150-800, indicating a complex chemical composition of aerosols from  
513 residential sources. CHO group was the most abundant component in the WSOC extracts and the  
514 contribution of CHO compounds to the total intensity in aerosols from raw biomass burning was  
515 significantly higher than those from biomass pellets and coal smokes. On the other hand, WISOC  
516 extract contained more SOCs, especially in the coal combustion aerosol. Notably, CHON  
517 compounds were more abundant in the coal combustion emissions, which was due to the higher fuel  
518 N content of coals ( $r = 0.936$ ,  $p < 0.05$ ). The SOCs emissions were more predominant in flaming  
519 phases, as positive correlation between SOCs abundance with the MCE values ( $r = 0.750$ ,  
520  $p < 0.05$ ). The CHO, CHON, and CHONS groups generated from coal combustion were characterized  
521 by high unsaturated level with more aromatic species, while CHOS groups had higher aromaticity  
522 degree in biomass smoke aerosols. It was found that MAE values were positively correlated with  
523 the CHOS condensed aromatics proportion for both WSOC ( $r = 0.714$ ,  $p < 0.05$ ) and WISOC extract  
524 ( $r = 0.929$ ,  $p < 0.001$ ). These results indicated that higher CHOS condense aromatics abundance in  
525 biomass burning aerosols could partly explain the higher MAE values of raw biomass smokes. The  
526 further analysis showed positive correlation of MAE with the CHOS condensed aromatics fractions  
527 which were the fraction simultaneously detected in all samples. These results indicated that light  
528 absorption capability of source aerosols may be due to the higher abundance of some CHOS  
529 aromatic compounds commonly emitted from both coal and biomass burning, rather than the unique  
530 tracers. The unique formulas of coal combustion aerosols were in the lower H/C and O/C regions  
531 with higher unsaturated compounds in the VK diagram. This work is potentially applicable to the



---

532 source appointment based on the molecular characteristics and to future studies developing more  
533 scientific control measures by focusing on one major component (e.g., CHOS condensed aromatics)  
534 of light absorption aerosols.

535 There are still some questions that need to be investigated in the future study. First, the study on  
536 BrC composition in this research used dissolved OC as a substitute. However, this substitute cannot  
537 fully represent BrC emissions. Both WSOC and WISOC contain some non-light-absorbing  
538 component, and the proportion of these components is unknown, making it difficult to measure the  
539 representativeness of extractable OC for BrC. Additionally, the lack of study about the emissions  
540 characteristics under controlled combustion conditions limits the obtained results. The controlled  
541 experiment including flaming or smoldering burns, air flow, and combustion temperature are needed  
542 in the future work. Third, fresh burning-derived OC released into the atmosphere can undergo  
543 various aging reactions such as photochemical degradation. These reactions can significantly alter  
544 the light absorptivity and chemical properties of BrC components. It is essential to consider the  
545 optical properties and lifetimes of organic compounds emitted from solid fuel combustion in climate  
546 models.

547 **Data availability.**

548 Data are available by contacting the corresponding authors

549 **Supplement**

550 The following information is in the appendix and available via the Internet:

551 Data processing in the ESI FT-ICR MS; fuel properties of coal and biomass fuels tested;  
552 number of formulas in each group, values of elemental ratios, MW, and DBE values in the WSOC  
553 and WISCO for each source type; Stoichiometric ranges of VK classes; Correlation between fuel N



---

554 and emission factors of NO<sub>x</sub>; the VK diagrams of WSOC and WISOC for different source samples;  
555 and correlations between the VK plots of WSOC/WISOC and fuel properties or combustion  
556 conditions.

#### 557 **Author contributions**

558 LZ, GS, and ST designed the experiment. LZ and JL prepared the filters used. LZ, YL, XL and  
559 ZL conducted the sample collection. LZ and JL performed the data analysis. LZ wrote the paper.  
560 GS, and ST reviewed and commented on the paper.

#### 561 **Competing interests**

562 The authors declare that they have no conflict of interest.

#### 563 **Acknowledgement**

564 Funding for this study was partly from National Natural Science Foundation of China  
565 (42077328, and 41922057). The authors greatly appreciated valuable help in data analyzing by Prof.  
566 Jianzhong Song from CAS.

#### 567 **Financial support**

568 This research has been supported by National Natural Science Foundation of China (42077328,  
569 and 41922057)

#### 570 **References**

571 Bianco, A., Deguillaume, L., Vaitilingom, M., Nicol, E., Baray, J.L., Chaumerliac, N., and  
572 Bridoux, M.: Molecular Characterization of Cloud Water Samples Collected at the Puy de Dome  
573 (France) by Fourier Transform Ion Cyclotron Resonance Mass Spectrometry, *Environ. Sci. Technol.*,  
574 52, 10275-10285, <https://doi.org/10.1021/acs.est.8b01964>, 2018.

575 Bond, T. C.: Spectral dependence of visible light absorption by carbonaceous particles emitted  
576 from coal combustion, *Geophys. Res. Lett.*, 28, 4075-4078, <https://doi.org/10.1029/2001GL013652>,  
577 2001.

578 Bond, T. C. and Bergstrom, R. W.: Light absorption by carbonaceous particles: An investigative  
579 review, *Aerosol Sci. Technol.*, 40, 27-67, <https://doi.org/10.1080/02786820500421521>, 2006.



- 580 Brege, M., Paglione, M., Gilardoni, S., Decesari, S., Facchini, M. C., and Mazzoleni, L. R.:  
581 Molecular insights on aging and aqueous-phase processing from ambient biomass burning  
582 emissions-influenced Po Valley fog and aerosol, *Atmos. Chem. Phys.*, 18, 13197-13214,  
583 <https://doi.org/10.5194/acp-18-13197-2018>, 2018.
- 584 Burling, I. R., Yokelson, R. J., Griffith, D. W. T., Johnson, T. J., Veres, P., Roberts, J. M.,  
585 Warneke, C., Urbanski, S. P., Reardon, J., Weise, D. R., Hao, W. M., and de Gouw, J.: Laboratory  
586 measurements of trace gas emissions from biomass burning of fuel types from the southeastern and  
587 southwestern United States, *Atmos. Chem. Phys.*, 10, <https://doi.org/10.5194/acp-10-11115-2010>,  
588 2010.
- 589 Cao, T., Li, M., Zou, C., Fan, X., Song, J., Jia, W., Yu, C., Yu, Z., and Peng, P.: Chemical  
590 composition, optical properties, and oxidative potential of water- and methanol-soluble organic  
591 compounds emitted from the combustion of biomass materials and coal, *Atmos. Chem. Phys.*, 21,  
592 13187-13205, <https://doi.org/10.5194/acp-21-13187-2021>, 2021.
- 593 Chen, Y. and Bond, T. C.: Light absorption by organic carbon from wood combustion, *Atmos.*  
594 *Chem. Phys.*, 10, 1773-1787, <https://doi.org/10.5194/acp-10-1773-2010>, 2010.
- 595 Du, Z., He, K., Cheng, Y., Duan, F., Ma, Y., Liu, J., Zhang, X., Zheng, M., and Weber, R.: A  
596 yearlong study of water-soluble organic carbon in Beijing II: Light absorption properties, *Atmos.*  
597 *Environ.*, 89, 235-241, <https://doi.org/10.1016/j.atmosenv.2014.02.022>, 2014.
- 598 Fan, X., Li, M., Cao, T., Cheng, C., Li, F., Xie, Y., Wei, S., Song, J., and Peng, P. a.: Optical  
599 properties and oxidative potential of water-and alkaline-soluble brown carbon in smoke particles  
600 emitted from laboratory simulated biomass burning, *Atmos. Environ.*, 194, 48-57,  
601 <https://doi.org/10.1016/j.atmosenv.2018.09.025>, 2018.
- 602 Feng, Y., Ramanathan, V., and Kotamarthi, V. R.: Brown carbon: a significant atmospheric  
603 absorber of solar radiation? *Atmos. Chem. Phys.*, 13, 8607-8621, <https://doi.org/10.5194/acp-13-8607-2013>, 2013.
- 605 Hansson, K. M., Samuelsson, J., Tullin, C., and Amand, L. E.: Formation of HNCO, HCN, and  
606 NH<sub>3</sub> from the pyrolysis of bark and nitrogen-containing model compounds, *Combust. Flame*, 137,  
607 265-277, <https://doi.org/10.1016/j.combustflame.2004.01.005>, 2004.
- 608 He, T., Wu, Y., Wang, D., Cai, J., Song, J., Yu, Z., Zeng, X., and Peng, P. a.: Molecular  
609 compositions and optical properties of water-soluble brown carbon during the autumn and winter in  
610 Guangzhou, China, *Atmos. Environ.*, 296, <https://doi.org/10.1016/j.atmosenv.2022.119573>, 2023.
- 611 Holder, A. L., Hagler, G. S. W., Aurell, J., Hays, M. D., and Gullett, B. K.: Particulate matter  
612 and black carbon optical properties and emission factors from prescribed fires in the southeastern  
613 United States, *J. Geophys. Res.: Atmos.*, 121, 3465-3483, <https://doi.org/10.1002/2015JD024321>,  
614 2016.
- 615 Huang, R.J., Yang, L., Cao, J., Chen, Y., Chen, Q., Li, Y., Duan, J., Zhu, C., Dai, W., Wang, K.,  
616 Lin, C., Ni, H., Corbin, J. C., Wu, Y., Zhang, R., Tie, X., Hoffmann, T., O'Dowd, C., and Dusek, U.:  
617 Brown Carbon Aerosol in Urban Xi'an, Northwest China: The Composition and Light Absorption  
618 Properties, *Environ. Sci. Technol.*, 52, 6825-6833, <https://doi.org/10.1021/acs.est.8b02386>, 2018.
- 619 Huang, R.J., Yang, L., Shen, J., Yuan, W., Gong, Y., Guo, J., Cao, W., Duan, J., Ni, H., Zhu, C.,  
620 Dai, W., Li, Y., Chen, Y., Chen, Q., Wu, Y., Zhang, R., Dusek, U., O'Dowd, C., and Hoffmann, T.:  
621 Water-Insoluble Organics Dominate Brown Carbon in Wintertime Urban Aerosol of China:  
622 Chemical Characteristics and Optical Properties, *Environ. Sci. Technol.*, 54, 7836-7847,  
623 <https://doi.org/10.1021/acs.est.0c01149>, 2020.
- 624 Huo, Y., Li, M., Jiang, M., and Qi, W.: Light absorption properties of HULIS in primary  
625 particulate matter produced by crop straw combustion under different moisture contents and  
626 stacking modes, *Atmos. Environ.*, 191, 490-499, <https://doi.org/10.1016/j.atmosenv.2018.08.038>,  
627 2018.



- 628 Jen, C. N., Hatch, L. E., Selimovic, V., Yokelson, R. J., Weber, R., Fernandez, A. E., Kreisberg,  
629 N. M., Barsanti, K. C., and Goldstein, A. H.: Speciated and total emission factors of particulate  
630 organics from burning western US wildland fuels and their dependence on combustion efficiency,  
631 *Atmos. Chem. Phys.*, 19, 1013-1026, <https://doi.org/10.5194/acp-19-1013-2019>, 2019.
- 632 Jiang, B., Kuang, B. Y., Liang, Y., Zhang, J., Huang, X. H. H., Xu, C., Yu, J. Z., and Shi, Q.:  
633 Molecular composition of urban organic aerosols on clear and hazy days in Beijing: a comparative  
634 study using FT-ICR MS, *Environ. Chem.*, 13, 888-901, <https://doi.org/10.1071/EN15230>, 2016.
- 635 Jiang, H., Li, J., Sun, R., Tian, C., Tang, J., Jiang, B., Liao, Y., Chen, C.-E., and Zhang, G.:  
636 Molecular Dynamics and Light Absorption Properties of Atmospheric Dissolved Organic Matter,  
637 *Environ. Sci. Technol.*, 55, 10268-10279, <https://doi.org/10.1021/acs.est.1c01770>, 2021.
- 638 Jo, D. S., Park, R. J., Lee, S., Kim, S.-W., and Zhang, X.: A global simulation of brown carbon:  
639 implications for photochemistry and direct radiative effect, *Atmos. Chem. Phys.*, 16, 3413-3432,  
640 <https://doi.org/10.5194/acp-16-3413-2016>, 2016.
- 641 Laskin, A., Laskin, J., and Nizkorodov, S. A.: Chemistry of Atmospheric Brown Carbon, *Chem.*  
642 *Rev.*, 115, 4335-4382, <https://doi.org/10.1021/cr5006167>, 2015.
- 643 Laskin, A., Smith, J. S., and Laskin, J.: Molecular Characterization of Nitrogen-Containing  
644 Organic Compounds in Biomass Burning Aerosols Using High-Resolution Mass Spectrometry,  
645 *Environ. Sci. Technol.*, 43, 3764-3771, <https://doi.org/10.1021/es803456n>, 2009.
- 646 Li, J., Zhang, Q., Wang, G., Li, J., Wu, C., Liu, L., Wang, J., Jiang, W., Li, L., Ho, K. F., and  
647 Cao, J.: Optical properties and molecular compositions of water-soluble and water-insoluble brown  
648 carbon (BrC) aerosols in northwest China, *Atmos. Chem. Phys.*, 20, 4889-4904,  
649 <https://doi.org/10.5194/acp-20-4889-2020>, 2020.
- 650 Li, M., Fan, X., Zhu, M., Zou, C., Song, J., Wei, S., Jia, W., and Peng, P. a.: Abundance and  
651 Light Absorption Properties of Brown Carbon Emitted from Residential Coal Combustion in China,  
652 *Environ. Sci. Technol.*, 53, 595-603, <https://doi.org/10.1021/acs.est.8b05630>, 2019.
- 653 Lin, P., Rincon, A. G., Kalberer, M., and Yu, J. Z.: Elemental Composition of HULIS in the  
654 Pearl River Delta Region, China: Results Inferred from Positive and Negative Electrospray High  
655 Resolution Mass Spectrometric Data, *Environ. Sci. Technol.*, 46, 7454-7462,  
656 <https://doi.org/10.1021/es300285d>, 2012.
- 657 Lv, J., Zhang, S., Wang, S., Luo, L., Cao, D., and Christie, P.: Molecular-Scale Investigation  
658 with ESI-FT-ICR-MS on Fractionation of Dissolved Organic Matter Induced by Adsorption on Iron  
659 Oxyhydroxides, *Environ. Sci. Technol.*, 50, 2328-2336, <https://doi.org/10.1021/acs.est.5b04996>,  
660 2016.
- 661 McMeeking, G. R., Kreidenweis, S. M., Baker, S., Carrico, C. M., Chow, J. C., Collett, J. L.,  
662 Jr., Hao, W. M., Holden, A. S., Kirchstetter, T. W., Malm, W. C., Moosmueller, H., Sullivan, A. P.,  
663 and Wold, C. E.: Emissions of trace gases and aerosols during the open combustion of biomass in  
664 the laboratory, *J. Geophys. Res.: Atmos.*, 114, <https://doi.org/10.1029/2009JD011836>, 2009.
- 665 Mo, Y., Li, J., Liu, J., Zhong, G., Cheng, Z., Tian, C., Chen, Y., and Zhang, G.: The influence  
666 of solvent and pH on determination of the light absorption properties of water-soluble brown carbon,  
667 *Atmos. Environ.*, 161, 90-98, <https://doi.org/10.1016/j.atmosenv.2017.04.037>, 2017.
- 668 Mo, Y., Zhong, G., Li, J., Liu, X., Jiang, H., Tang, J., Jiang, B., Liao, Y., Cheng, Z., and Zhang,  
669 G.: The Sources, Molecular Compositions, and Light Absorption Properties of Water-Soluble  
670 Organic Carbon in Marine Aerosols From South China Sea to the Eastern Indian Ocean, *J. Geophys.*  
671 *Res.: Atmos.*, 127, <https://doi.org/10.1029/2021JD036168>, 2022.
- 672 Olson, M. R., Garcia, M. V., Robinson, M. A., Van Rooy, P., Dietenberger, M. A., Bergin, M.,  
673 and Schauer, J. J.: Investigation of black and brown carbon multiple-wavelength-dependent light  
674 absorption from biomass and fossil fuel combustion source emissions, *J. Geophys. Res.: Atmos.*,  
675 120, 6682-6697, <https://doi.org/10.1002/2014JD022970>, 2015.



- 676 Park, S. S. and Yu, J.: Chemical and light absorption properties of humic-like substances from  
677 biomass burning emissions under controlled combustion experiments, *Atmos. Environ.*, 136, 114-  
678 122, <https://doi.org/10.1016/j.atmosenv.2016.04.022>, 2016.
- 679 Patriarca, C., Bergquist, J., Sjoberg, P. J. R., Tranvik, L., and Hawkes, J. A.: Online HPLC-  
680 ESI-HRMS Method for the Analysis and Comparison of Different Dissolved Organic Matter  
681 Samples, *Environ. Sci. Technol.*, 52, 2091-2099, <https://doi.org/10.1021/acs.est.7b04508>, 2018.
- 682 Pokhrel, R. P., Wagner, N. L., Langridge, J. M., Lack, D. A., Jayarathne, T., Stone, E. A.,  
683 Stockwell, C. E., Yokelson, R. J., and Murphy, S. M.: Parameterization of single-scattering albedo  
684 (SSA) and absorption Angstrom exponent (AAE) with EC / OC for aerosol emissions from biomass  
685 burning, *Atmos. Chem. Phys.*, 16, 9549-9561, [10.5194/acp-16-9549-2016](https://doi.org/10.5194/acp-16-9549-2016), 2016.
- 686 Rathod, T., Sahu, S. K., Tiwari, M., Yousaf, A., Bhangare, R. C., and Pandit, G. G.: Light  
687 Absorbing Properties of Brown Carbon Generated from Pyrolytic Combustion of Household  
688 Biofuels, *Aerosol Air Qual. Res.*, 17, 108-116, [10.4209/aaqr.2015.11.0639](https://doi.org/10.4209/aaqr.2015.11.0639), 2017.
- 689 Reisen, F., Meyer, C. P., Weston, C. J., and Volkova, L.: Ground-Based Field Measurements of  
690 PM<sub>2.5</sub> Emission Factors From Flaming and Smoldering Combustion in Eucalypt Forests, *J.  
691 Geophys. Res.: Atmos.*, 123, 8301-8314, <https://doi.org/10.1029/2018JD028488>, 2018.
- 692 Ren, Q. and Zhao, C.: Evolution of fuel-N in gas phase during biomass pyrolysis, *Renewable  
693 Sustainable Energy Rev.*, 50, 408-418, <https://doi.org/10.1016/j.rser.2015.05.043>, 2015.
- 694 Saleh, R., Robinson, E. S., Tkacik, D. S., Ahern, A. T., Liu, S., Aiken, A. C., Sullivan, R. C.,  
695 Presto, A. A., Dubey, M. K., Yokelson, R. J., Donahue, N. M., and Robinson, A. L.: Brownness of  
696 organics in aerosols from biomass burning linked to their black carbon content, *Nat. Geosci.*, 7, 647-  
697 650, [10.1038/ngeo2220](https://doi.org/10.1038/ngeo2220), 2014.
- 698 Song, J., Li, M., Jiang, B., Wei, S., Fan, X., and Peng, P. a.: Molecular Characterization of  
699 Water-Soluble Humic like Substances in Smoke Particles Emitted from Combustion of Biomass  
700 Materials and Coal Using Ultrahigh-Resolution Electrospray Ionization Fourier Transform Ion  
701 Cyclotron Resonance Mass Spectrometry, *Environ. Sci. Technol.*, 52, 2575-2585,  
702 <https://doi.org/10.1021/acs.est.7b06126>, 2018.
- 703 Song, J., Li, M., Fan, X., Zou, C., Zhu, M., Jiang, B., Yu, Z., Jia, W., Liao, Y., and Peng, P. a.:  
704 Molecular Characterization of Water- and Methanol-Soluble Organic Compounds Emitted from  
705 Residential Coal Combustion Using Ultrahigh-Resolution Electrospray Ionization Fourier  
706 Transform Ion Cyclotron Resonance Mass Spectrometry, *Environ. Sci. Technol.*, 53, 13607-13617,  
707 <https://doi.org/10.1021/acs.est.9b04331>, 2019.
- 708 Sun, J. Z., Zhi, G. R., Hitznerberger, R., Chen, Y. J., Tian, C. G., Zhang, Y. Y., Feng, Y. L.,  
709 Cheng, M. M., Zhang, Y. Z., Cai, J., Chen, F., Qiu, Y., Jiang, Z., Li, J., Zhang, G., and Mo, Y.:  
710 Emission factors and light absorption properties of brown carbon from household coal combustion  
711 in China, *Atmos. Chem. Phys.*, 17, 4769-4780, <https://doi.org/10.5194/acp-17-4769-2017>, 2017.
- 712 Tang, J., Li, J., Su, T., Han, Y., Mo, Y., Jiang, H., Cui, M., Jiang, B., Chen, Y., Tang, J., Song,  
713 J., Peng, P. a., and Zhang, G.: Molecular compositions and optical properties of dissolved brown  
714 carbon in biomass burning, coal combustion, and vehicle emission aerosols illuminated by  
715 excitation-emission matrix spectroscopy and Fourier transform ion cyclotron resonance mass  
716 spectrometry analysis, *Atmos. Chem. Phys.*, 20, 2513-2532, [https://doi.org/10.5194/acp-20-2513-  
717 2020](https://doi.org/10.5194/acp-20-2513-2020), 2020.
- 718 Wang, Q. Q., Zhou, Y. Y., Ma, N., Zhu, Y., Zhao, X. C., Zhu, S. W., Tao, J. C., Hong, J., Wu,  
719 W. J., Cheng, Y. F., and Su, H.: Review of Brown Carbon Aerosols in China: Pollution Level, Optical  
720 Properties, and Emissions, *J. Geophys. Res.: Atmos.*, 127, <https://doi.org/10.1029/2021JD035473>,  
721 2022.
- 722 Wei, W., Xie, Q., Yan, Q., Hu, W., Chen, S., Su, S., Zhang, D., Wu, L., Huang, S., Zhong, S.,  
723 Deng, J., Yang, T., Li, J., Pan, X., Wang, Z., Sun, Y., Kong, S., and Fu, P.: Dwindling aromatic





- 724 compounds in fine aerosols from chunk coal to honeycomb briquette combustion, *Sci. Total*  
725 *Environ.*, 838, <https://doi.org/10.1016/j.scitotenv.2022.155971>, 2022.
- 726 Wozniak, A. S., Bauer, J. E., Sleighter, R. L., Dickhut, R. M., and Hatcher, P. G.: Technical  
727 Note: Molecular characterization of aerosol-derived water soluble organic carbon using ultrahigh  
728 resolution electrospray ionization Fourier transform ion cyclotron resonance mass spectrometry,  
729 *Atmos. Chem. Phys.*, 8, 5099-5111, <https://doi.org/10.5194/acp-8-5099-2008>, 2008.
- 730 Xie, M. J., Hays, M. D., and Holder, A. L.: Light-absorbing organic carbon from prescribed  
731 and laboratory biomass burning and gasoline vehicle emissions, *Sci. Rep.*, 7,  
732 <https://doi.org/10.1038/s41598-017-06981-8>, 2017.
- 733 Xiong, R., Li, J., Zhang, Y., Zhang, L., Jiang, K., Zheng, H., Kong, S., Shen, H., Cheng, H.,  
734 Shen, G., and Tao, S.: Global brown carbon emissions from combustion sources, *Environ. Sci.*  
735 *Ecotechnology*, 12, 100201, <https://doi.org/10.1016/j.ese.2022.100201>, 2022.
- 736 Yokelson, R. J., Susott, R., Ward, D. E., Reardon, J., and Griffith, D. W. T.: Emissions from  
737 smoldering combustion of biomass measured by open-path Fourier transform infrared spectroscopy,  
738 *J. Geophys. Res.: Atmos.*, 102, 18865-18877, [10.1029/97jd00852](https://doi.org/10.1029/97jd00852), 1997.
- 739 Yue, S., Zhu, J., Chen, S., Xie, Q., Li, W., Li, L., Ren, H., Su, S., Li, P., Ma, H., Fan, Y., Cheng,  
740 B., Wu, L., Deng, J., Hu, W., Ren, L., Wei, L., Zhao, W., Tian, Y., Pan, X., Sun, Y., Wang, Z., Wu,  
741 F., Liu, C.-Q., Su, H., Penner, J. E., Pöschl, U., Andreae, M. O., Cheng, Y., and Fu, P.: Brown carbon  
742 from biomass burning imposes strong circum-Arctic warming, *One Earth*, 5, 293-304,  
743 <https://doi.org/10.1016/j.oneear.2022.02.006>, 2022.
- 744 Zhang, L., Luo, Z., Du, W., Li, G., Shen, G., Cheng, H., and Tao, S.: Light absorption properties  
745 and absorption emission factors for indoor biomass burning, *Environ. Pollut.*, 267,  
746 <https://doi.org/10.1016/j.envpol.2020.115652>, 2020.
- 747 Zhang, L., Luo, Z. H., Li, Y. J., Chen, Y. C., Du, W., Li, G., Cheng, H. F., Shen, G. F., and Tao,  
748 S.: Optically Measured Black and Particulate Brown Carbon Emission Factors from Real-World  
749 Residential Combustion Predominantly Affected by Fuel Differences, *Environ. Sci. Technol.*, 55,  
750 169-178, <https://doi.org/10.1021/acs.est.0c04784>, 2021a.
- 751 Zhang, L., Luo, Z., Xiong, R., Liu, X., Li, Y., Du, W., Chen, Y., Pan, B., Cheng, H., Shen, G.,  
752 and Tao, S.: Mass Absorption Efficiency of Black Carbon from Residential Solid Fuel Combustion  
753 and Its Association with Carbonaceous Fractions, *Environ. Sci. Technol.*, 55, 10662-10671,  
754 <https://doi.org/10.1021/acs.est.1c02689>, 2021b.
- 755 Zhang, L., Hu, B., Liu, X., Luo, Z., Xing, R., Li, Y., Xiong, R., Li, G., Cheng, H., Lu, Q., Shen,  
756 G., and Tao, S.: Variabilities in Primary N-Containing Aromatic Compound Emissions from  
757 Residential Solid Fuel Combustion and Implications for Source Tracers, *Environ. Sci. Technol.*,  
758 <https://doi.org/10.1021/acs.est.2c03000>, 2022.
- 759 Zhao, Y., Hallar, A. G., and Mazzoleni, L. R.: Atmospheric organic matter in clouds: exact  
760 masses and molecular formula identification using ultrahigh-resolution FT-ICR mass spectrometry,  
761 *Atmos. Chem. Phys.*, 13, 12343-12362, <https://doi.org/10.5194/acp-13-12343-2013>, 2013.
- 762
- 763